

Lunar Swirl Formation in an Irregular-Shaped Dusty Plasma Medium. C. Carmichael, G. Griffin, M. Cook, Lorin Matthews, and T. W. Hyde, Center for Astrophysics, Space Physics and Engineering Research, One Bear Place #97283, Baylor University, Waco, TX, 76798-7283, USA.

Introduction: Lunar swirls are high albedo sweeping patterns spread across the lunar surface varying in length from 1-5 kilometers. Swirls are located near or on magnetic anomalies. The formation of lunar swirls has been intensely studied and a single theory has not been named as a catalyst for the swirls. A few viable theories have been proposed, for example, the Cometary Impact model and Dust Shielding model. This work examines swirl formation in the dust transport model. In this model, the incoming plasma (solar winds) charge the dust grains on the surface. The interaction between the magnetic field and the charged grains can cause the regolith to be sorted and preferentially accumulate into the swirl patterns seen on the lunar surface [1, 2, 3, 4].

In this work, we test the viability of the dust transport model in creating lunar swirl patterns experimentally employing a GEC RF Cell. Additionally, the characterization of charged dust dynamics in a magnetic field is also a possible avenue for establishing dust mitigation techniques. Dust mitigation is essential for upcoming lunar missions.

Method: Recent research suggests that the geometry of the underlying magnetic sources for the formation of lunar swirls must be constrained to certain limits: the anomaly source depth cannot be greater than the transition length L (figure 1), the width of the swirl can never exceed twice the transition length and the sources of the magnetization must be both narrow and shallow in order to produce a swirl. These conditions are implied from necessary rock magnetizations, the origin of the lunar rock's natural remnant magnetization, and the sinuous morphology of lunar swirl complexes [3].

These constraints imply that the source of such surface magnetic anomalies could be caused by dikes or lava tubes [3]. In this case, magnetic anomalies were simulated using shallow dipole magnets, arranged similarly to known swirl patterns. All magnet formations were made in accordance with the geometric constraints listed previously and placed in Teflon plates.

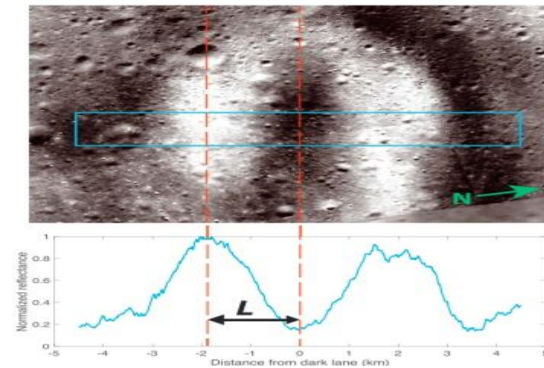


Figure 1: The transition length L is the distance between highest and lowest albedo for each swirl. Constraints imposed by this research [2] dictated the dimensions of the magnet formations.

Using a Gaseous Electronics Conference Radiofrequency Cell (see figure 2), an Argon plasma was produced employing a RF source. Experiments were performed at 5-25 Watts, for pressures ranging from 20-120 mTorr. Laser fans or backlights were used to illuminate the regolith simulant particles depending on reflectivity of the grains [5]. Regolith simulants used included: JSC-1 (100 microns), Lunar Mare (63 microns), & Lunar Highland (90 microns), with varying mean radii particle size and mineral compositions.

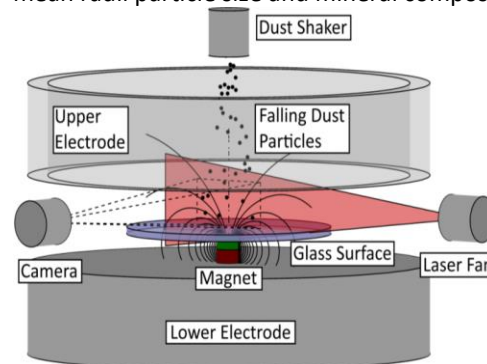


Figure 2: Inner chamber of the GEC RF Cell [2].

Dust particles dropped through the argon plasma accumulated charge. The charged falling dust grains were tracked using a Fastcam Mini UX50. The resulting data allowed the accelerations of the dust grains to be calculated with their resulting forces determined from the parameters of the plasma. The accelerations and velocities of the falling dust were plotted (figure 3) using data from a particle tracker in MOSAIC.

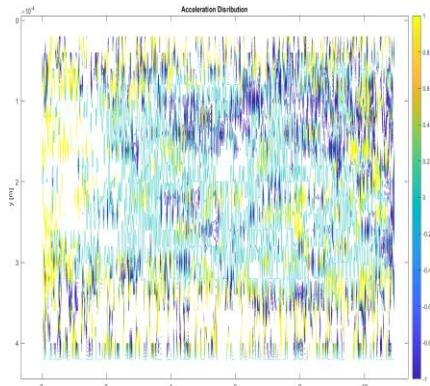


Figure 3: The plot shows the areas of highest and lowest acceleration. The particles travel from left to right.

Equation 1 shows the possible forces involved for dust particles.

$$(1) \mathbf{F}^g + \mathbf{F}^b + \mathbf{F}^e + \mathbf{F}^t + \mathbf{F}^i + \mathbf{F}^n = M\mathbf{a}$$

The forces listed in equation 1 are, \mathbf{F}^g (Gravity), \mathbf{F}^b (Magnetic field force), \mathbf{F}^e (electric field force), \mathbf{F}^t (thermophoretic force), the two drag forces \mathbf{F}^i (ion drag), & \mathbf{F}^n (neutral drag).

Results: Two magnet formations were used for each of the regolith simulants tested. We note here that the smaller particle sizes had an easier time forming swirl patterns compared to larger sized dusts. JSC-1 was the most effective simulant at forming the patterns. This may be due to JSC-1 having a larger distribution of particle sizes compared to the other simulants. A reproduced “negative” of the Reiner Gamma lunar swirl is shown in figure 4.

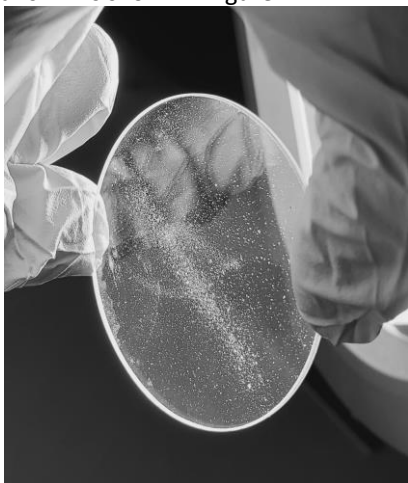


Figure 4: Swirl reproduction using JSC-1, the large line of dust is caused by the trajectory of the dust dropper across the plate.

Future Work: Additional formations of lunar swirls have been manufactured and will be tested to see if different shapes of lunar swirls can be reproduced.

Furthermore, the axial magnetization of the dipole magnets caused accumulations of particles in potential wells due to the placement of the magnets in the Teflon plates. Later experiments could include sideways orientation of the magnets instead of flat placement to avoid these build ups of particles. Figure 5 shows how the dust can get caught in potential wells above a dipole magnet.

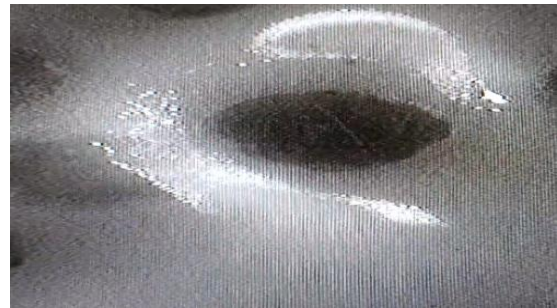


Figure 5: Dust “in-transit” to another potential well above a dipole magnet. Dust pictured is JSC-1.

Conclusion: In this work, we investigated the dynamics of charged dust grains traveling in a magnetic field, examined the reproduction of the Reiner Gamma lunar swirl and observed the interaction between plasma and magnetic anomalies. Possible measurements of lunar surface conditions could lead to magnetic field line extrapolation as well as particle charge from trajectory data. Observing how charged dust travels along magnetic field lines could be a step towards the development of advanced dust mitigation techniques in the future.

Acknowledgement: This material is based upon work supported by NASA JPL & NASA under Grants No. EW-2962-LDRM and 20_EW20_2-0053.

References: [1] Hemingway, D., and I. Garrick-Bethell (2012), *Journal of Geophysical Research*, 117, E10012. [2] Droppmann, M., Laufer, R., Herdrich, G., Matthews, L.S., Hyde, T.W. (2015). *Physical Review*, E 92, 023107. [3] Hemingway, D. J., & Tikoo, S. M. (2018). *Journal of Geophysical Research: Planets*, 123 [4]. Denevi, B.W., Robinson, M.S., Boyd, A.K., Blewett, D.T., Klimaa, R.L. (2016) *Elsevier, Icarus*, 273, p. 53-67. [5] Creel, J.R., Characteristic Measurements within a GEC rf Reference Cell (2010). *Baylor University*